Displacement Estimation for Different Gait Patterns in Micro-Sensor Motion Capture

Xiaoli Meng*, Guanhong Tao*, Zhiqiang Zhang†, Shuyan Sun*, Jiankang Wu* and Wai-Choong Wong‡
*Graduate University of Chinese Academy of Sciences (GUCAS), Beijing, China
†Department of Computing, Imperial College London, UK
‡Department of Electrical and Computer Engineering, National University of Singapore (NUS), Singapore
Email: mengxiaoli07@mails.gucas.ac.cn

***Abstract*—The human body displacement estimation in different gait patterns using wearable sensors is extremely challenging due to lack of external references. In this paper, we present a novel algorithm to estimate the Center of Mass (CoM) displacement of human body during walking, running and hopping using 7 body-worn Sensor Measurement Units (SMUs). The lower body posture and feet displacements are firstly estimated by a complementary Kalman filter (CKF) which compensates the orientation, velocity and position errors of the Inertial Navigation system (INS) solutions through its error state vector. The CoM displacement can then be acquired by further fusion of the lower body posture and feet locations based on the linked biomechanical model. The experimental results have shown that our method can accurately capture human motion including orientation and locomotion for these three different gait patterns with regard to the optical motion tracker.**

***Index Terms*—Displacement estimation, Complementary Kalman filter, Human biomechanical model, Motion capture.**

I. Introduction

Human gait analysis and lower limb motion capture have been widely used for animation, physical therapy, bio-engineering, neurology and rehabilitation. With rapid technological advances in Micro-electro-mechanical systems (MEMS), Sensor Measurement Units (SMUs, consisting of micro accelerometers, gyroscopes and magnetometers) are increasingly being used in human motion capture systems because of their compact size and ubiquitous deployment [1]–[4]. SMUs can be attached to body segments to measure the orientations of the body segments via fusion of sensor measurements. Based on the estimated orientations and the biomechanical characteristics of human body, the posture of the whole body can be obtained. Unfortunately, the subject's location within a global coordinate system cannot be reliably recovered because there is no external reference in a self-contained micro-sensor based motion capture (MMocap) system.

Since low-cost MEMS sensors are subject to significant random noise and bias, the subject's displacement estimation in space remains as a challenge in MMocap systems. There is some current work attempting to solve the problem. Meng *et al.* [5] proposed to estimate the displacement of human walking based on a 3D human biomechanical model, and obtained good results for walking via applying the fact that there is always at least one foot in contact with the ground during walking. The method is not applicable for the CoM displacement estimation during running and hopping as there is a phase no foot contacting the ground at all. To estimate the CoM displacement during running and hopping, the most intuitive method is to detect no ground contact periods and estimate the CoM position using double integration method. Researchers have proposed several methods to detect the ground contact phase during movements. For example, Kazuki *et al.* [6] proposed to put four push button switches under the shoes (two switches under the toe and two switches under the heel). This method will increase the cost of the system, and make the system more complicated. Moreover, it cannot work robustly, such as, when people run in tiptoe, it might be quite difficult to detect the reference point correctly. Young [7] derived a formula that the hip velocity is the opposite of the anchor joint, which stays stationary on the ground during movements. The hip velocity can be calculated from integration of acceleration, but the integration will bring drifts. If the anchor joint exists, the velocity of the anchor joint is used to update the hip velocity; and if not, the hip velocity will be used directly to get the position of the hip. However, the formula is broken as the anchor is transferred between joints during movements. Yun *et al.* [8] described a method for using accelerometer data combined with orientation estimated from the same sensor module to calculate the position during walking and running. The periodic nature of these motions includes short periods of zero foot velocity when the foot is stationary on the ground. This pattern allows for precise drift error correction. Relative position is calculated through double integration of the accelerometer data. They got some preliminary results for running outside in a straight line. Despite these efforts, significant problems still remain.

In this paper, we propose an algorithm to estimate the CoM displacement for different gait patterns, including walking, running and hopping. 7 SMUs are placed on the lower body segments to get their orientations and the displacements of both feet, which are achieved by a complementary Kalman filter (CKF). The CKF compensates the orientation, velocity and position errors of the Inertial Navigation system (INS) solutions through its error state vector. Zero velocity update (ZUPT) is also employed to restrict the fast growing drifts during integration for feet displacements estimation. The CoM displacement can then be acquired by further fusion of the lower body orientation and feet locations based on the linked

biomechanical model. The proposed method makes it possible to capture full human motion including posture and locomotion accurately in an area of unlimited size with no supporting infrastructure.

The remainder of the paper is organized as follows: Section 2 presents the details of the proposed methods to estimate the CoM displacements for different gait patterns. Experimental methods and results are provided in Section 3. Finally, conclusion and future work of this study are given in Section 4.

II. Proposed algorithm

The orientations of the SMUs and body segments are represented by quaternions. For relatively short time intervals, the discrete-time process model for quaternion [9] can be expressed as

$$q_t = \exp\left(\frac{1}{2}\Omega(\vec{\omega}_t)\Delta t\right) q_{t-1} \tag{1}$$

where q_t consists of a vector part $\vec{e}_t = [q_{1,t}, q_{2,t}, q_{3,t}]^{\mathrm{T}} \in \Re^3$ and a scalar part $q_{4,t} \in \Re$, i.e. $q_t = \left[\vec{e}_t^{\mathrm{T}}, q_{4,t}\right]^{\mathrm{T}} = [q_{1,t}, q_{2,t}, q_{3,t}, q_{4,t}]^{\mathrm{T}}$, and the superscript 'T' denotes transpose. Hereafter quaternion is defined as the orientation of the SMUs relative to the global frame unless otherwise specified. $\vec{\omega}_t = [\omega_{X,t}, \omega_{Y,t}, \omega_{Z,t}]^{\mathrm{T}}$ is the angular rate, Δt is the sampling interval, $\Omega(\vec{\omega}_t)$ is a 4×4 skew symmetric matrix as in

$$\Omega(\vec{\omega}_t) = \begin{bmatrix} -[\vec{\omega}_t \times] & \vec{\omega}_t \\ -\vec{\omega}_t^{\mathrm{T}} & 0 \end{bmatrix}, \tag{2}$$

and $[\vec{\omega}_t \times]$ represents the cross product operator.

Displacement can be estimated by double integration of the body acceleration represented in the global frame, denoted by $\vec{a}_t^{\mathrm{G}}$, as in

$$\begin{aligned} \vec{v}_t &= \vec{v}_{t-1} + \vec{a}_t^{\mathrm{G}} \Delta t \\ \vec{p}_t &= \vec{p}_{t-1} + \vec{v}_t \Delta t. \end{aligned} \tag{3}$$

Since the accelerometer signal $\vec{y}_{\mathrm{A,t}}$ consists of a body acceleration component $\vec{a}_t$ and a gravitational acceleration component $\vec{g}_t$, gravitational acceleration must be removed before integration. The orientations of the sensor relative to the global frame q_t can be used to get the linear acceleration by

$$\vec{a}_t^{\mathrm{G}} = A(q_t)\vec{y}_{\mathrm{A},t} - \vec{g}_0 \tag{4}$$

where $A(q_t)$ is the direction cosine matrix in terms of a quaternion between the sensor frame and global frame described by

$$A(q_t) = \left(q_{4,t}^2 - \vec{e}_t^{\mathrm{T}}\vec{e}_t\right)\mathbf{I_3} + 2\vec{e}_t\,\vec{e}_t^{\mathrm{T}} - 2q_{4,t}\,[\vec{e}_t \times] \tag{5}$$

and $\vec{g}_0$ is the gravitational acceleration in the global frame. However, it is difficult to remove the gravitational component clearly from the accelerometer signal. Any small error in $\vec{a}_t^{\mathrm{G}}$ can make the displacement error grow cubically over time.

The goal of this study is to estimate the CoM displacement to reconstruct the locomotion for human different gait patterns in MMocap system. Because of the unbounded drifts in the double integration process, the CoM displacement cannot be obtained by double integration of the acceleration data from the pelvis directly. This paper proposes to estimate the orientations of the lower body segments and displacement of both feet based on the INS mechanism first. ZUPT technique is imported when the feet are stationary on the ground to restrict the unbounded drifts of the feet displacements. Then the CoM displacements are estimated using the displacements of both feet and the orientations of lower body segments based on the human lower body biomechanical model. The hierarchical human model [10] is imported to eliminate the position error of each segment in relation to each other. The external ground contact update is further deployed to delimitate the displacement drifts. The schematic overview of the algorithm is shown in Fig. 1.

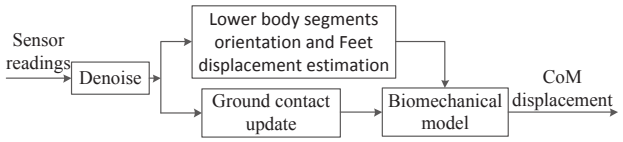

Fig. 1. The schematic overview of the proposed algorithm.

A. Sensor signal model

In our system, the SMU includes three types of sensors, namely accelerometer, gyroscope and magnetometer. The model of the measured gyroscope and accelerometer signals is given below.

1) Gyroscope: The gyroscope signal $\vec{y}_{\mathrm{G},t}$ is modeled as the sum of the angular rate $\vec{\omega}_t$, the bias $\vec{b}_{\mathrm{G},t}$, and a white noise term $\vec{w}_{\mathrm{G},t}$,

$$\vec{y}_{\mathrm{G},t} = \vec{\omega}_t + \vec{b}_{\mathrm{G},t} + \vec{w}_{\mathrm{G},t}. \tag{6}$$

The slow variation of the gyroscope bias is modeled as a first-order Markov process driven by a white Gaussian noise $\vec{u}_{\mathrm{bG},t}$, with covariance matrix Q_{bG},

$$\vec{b}_{\mathrm{G},t} = \vec{b}_{\mathrm{G},t-1} + \vec{u}_{\mathrm{bG},t}. \tag{7}$$

2) Accelerometer: The accelerometer signal $\vec{y}_{\mathrm{A},t}$ is modeled as the sum of the motion acceleration $\vec{a}_t$, the gravitational acceleration $\vec{g}_t$, the bias $\vec{b}_{\mathrm{A},t}$, and a white Gaussian noise term $\vec{w}_{\mathrm{A},t}$,

$$\vec{y}_{\mathrm{A},t} = \vec{a}_t + \vec{g}_t + \vec{b}_{\mathrm{A},t} + \vec{w}_{\mathrm{A},t}. \tag{8}$$

The slow variation of the accelerometer bias is modeled as a first-order Markov process driven by a white Gaussian noise $\vec{u}_{\mathrm{bA},t}$, with covariance matrix Q_{bA},

$$\vec{b}_{\mathrm{A},t} = \vec{b}_{\mathrm{A},t-1} + \vec{u}_{\mathrm{bA},t}. \tag{9}$$

B. Filter Structure

A CKF is designed to estimate the orientation and displacement for both feet, and orientation only for other segments, namely, femur, tibia and pelvis in the human lower body. The CKF operates on the errors of the state variables using a feedback structure. The flowchart of the CKF is given in Fig. 2. For the feet, the error states at time t for the filter are defined as $\delta\vec{x}_t = \left[\delta\vec{q}_t^{\mathrm{T}}, \vec{b}_{\mathrm{G},t}^{\mathrm{T}}, \delta\vec{p}_t^{\mathrm{T}}, \delta\vec{v}_t^{\mathrm{T}}, \vec{b}_{\mathrm{A},t}^{\mathrm{T}}\right]^{\mathrm{T}}$, including the vector part

of the error quaternion $\delta\vec{q}_t$, the gyroscope bias $\vec{b}_{\mathrm{G},t}$, the error position $\delta\vec{p}_t$, the error velocity $\delta\vec{v}_t$, and the acceleration bias $\vec{b}_{\mathrm{A},t}$. Each component has 3 elements, corresponding to a 15-dimensional estimation. For other segments in the lower body model, the error states are $\delta\vec{x}_t = \left[\delta\vec{q}_t^{\mathrm{T}}, \vec{b}_{\mathrm{G},t}^{\mathrm{T}}\right]^{\mathrm{T}}$, which is a 6-element vector.

The process model of the proposed filter is governed by

$$\delta\vec{x}_t = \mathbf{F_t}\delta\vec{x}_{t-1} + \vec{u}_t \tag{10}$$

where $\vec{u}_t$ is the process noise with covariance matrix $Q = E\left(\vec{u}_t\vec{u}_t^{\mathrm{T}}\right)$, and $\mathbf{F_t}$ is state transition matrix, which needs to be determined.

1) Quaternion error model: Define the true quaternion q_t as the composition of the estimated quaternion $\hat{q}_t$ and error quaternion δq_t

$$q_t = \hat{q}_t \otimes \delta q_t \tag{11}$$

where $\otimes$ is the quaternion multiplication. Due to δq_t denotes a small rotation, the scalar part of the quaternion will be close to 1, which can be written as $\delta q_t = \left[\delta\vec{q}_t^{\mathrm{T}}, 1\right]^{\mathrm{T}} = [\delta q_{t,1}, \delta q_{t,2}, \delta q_{t,3}, 1]^{\mathrm{T}}$. Thus we only include $\delta\vec{q}_t$ in the error state. The dynamic equation of the quaternion can be written as follows:

$$\dot{q}_t = \frac{1}{2} q_t \otimes \vec{\omega}_t = \frac{1}{2}\hat{q}_t \otimes \delta q_t \otimes \vec{\omega}_t, \tag{12a}$$

$$\dot{q}_t = \dot{\hat{q}}_t \otimes \delta q_t + \hat{q}_t \otimes \dot{\delta q}_t = \frac{1}{2}\hat{q}_t \otimes \vec{y}_{\mathrm{G},t} \otimes \delta q_t + \hat{q}_t \otimes \dot{\delta q}_t. \tag{12b}$$

From (12a) and (12b), we can get

$$\begin{aligned}\dot{\delta q}_t &= \frac{1}{2}(\delta q_t \otimes \vec{\omega}_t - \vec{y}_{\mathrm{G},t} \otimes \delta q_t) \\ &= \frac{1}{2}\left(\delta q_t \otimes \vec{y}_{\mathrm{G},t} - \vec{y}_{\mathrm{G},t} \otimes \delta q_t\right) - \frac{1}{2}\delta q_t \otimes \delta\vec{\omega}_t\end{aligned} \tag{13}$$

where $\delta\vec{\omega}_t = \vec{b}_{\mathrm{G},t} + \vec{w}_{\mathrm{G},t}$ as defined by (6). Let $\Upsilon(\vec{y}_{\mathrm{G},t})$ and $\Upsilon^{+}(\vec{y}_{\mathrm{G},t})$ denote the linear mappings for $\vec{y}_{\mathrm{G},t}$ from $\Re^3$ to $\Re^{4\times 4}$, as in $\Upsilon(\vec{y}_{\mathrm{G},t}) = \begin{bmatrix} -[\vec{y}_{\mathrm{G},t}\times] & -\vec{y}_{\mathrm{G},t} \\ \vec{y}_{\mathrm{G},t}^{\mathrm{T}} & 0 \end{bmatrix}$ and $\Upsilon^{+}(\vec{y}_{\mathrm{G},t}) = \begin{bmatrix} [\vec{y}_{\mathrm{G},t}\times] & -\vec{y}_{\mathrm{G},t} \\ \vec{y}_{\mathrm{G},t}^{\mathrm{T}} & 0 \end{bmatrix}$. Then we can get

$$\begin{bmatrix}\dot{\delta\vec{q}_t} \\ 0\end{bmatrix} = \frac{1}{2}\left(\Upsilon^{+}\left(\vec{y}_{\mathrm{G},t}\right)\delta q_t - \Upsilon\left(\vec{y}_{\mathrm{G},t}\right)\delta q_t\right) - \frac{1}{2}\delta q_t \otimes \delta\vec{\omega}_t \tag{14}$$

where $\delta q_t \otimes \delta\vec{\omega}_t = \delta\vec{\omega}_t + HOT(\delta q_t, \delta\vec{\omega}_t)$, and *HOT* stands for higher order terms. By neglecting the higher order terms, we can get

$$\begin{bmatrix}\dot{\delta\vec{q}_t} \\ 0\end{bmatrix} = \begin{bmatrix}\vec{y}_{\mathrm{G},t} \times \delta\vec{q}_t \\ 0\end{bmatrix} - \frac{1}{2}\begin{bmatrix}\vec{b}_{\mathrm{G},t} + \vec{w}_{\mathrm{G},t} \\ 0\end{bmatrix}. \tag{15}$$

The dynamics of the error quaternion can be written as:

$$\dot{\delta\vec{q}_t} = [\vec{y}_{\mathrm{G},t}\times]\,\delta\vec{q}_t - \frac{1}{2}\left(\vec{b}_{\mathrm{G},t} + \vec{w}_{\mathrm{G},t}\right), \tag{16}$$

thus the dynamics of the error quaternion can be integrated as:

$$\delta\vec{q}_t = \left(\mathbf{I_3} + \Delta t\,[\vec{y}_{\mathrm{G},t}\times]\right)\delta\vec{q}_{t-1} - \frac{1}{2}\Delta t\vec{b}_{\mathrm{G},t-1} - \vec{u}_{\mathrm{G},t} \tag{17}$$

where $\mathbf{I_3}$ is a 3×3 identity matrix, and $\vec{u}_{\mathrm{G},t} = \frac{1}{2}\Delta t\vec{w}_{\mathrm{G},t-1}$ is the zero mean Gaussian noise, with covariance matrix Q_{q}.

2) Velocity error model: To get the dynamics of the velocity errors, we start with the true body acceleration, denoted by $\dot{\vec{v}}_t$:

$$\dot{\vec{v}}_t = A(q_t)\vec{y}'_{\mathrm{A},t} - \vec{g}_0 = A(\hat{q}_t)C(\delta q_t)\vec{y}'_{\mathrm{A},t} - \vec{g}_0. \tag{18}$$

The estimated body acceleration, denoted by $\dot{\hat{\vec{v}}}_t$, is expressed as

$$\dot{\hat{\vec{v}}}_t = A(\hat{q}_t)\vec{y}_{\mathrm{A},t} - \vec{g}_0. \tag{19}$$

The difference between the true and estimated acceleration is computed by

$$\begin{aligned}\dot{\delta\vec{v}}_t &= \dot{\hat{\vec{v}}}_t - \dot{\vec{v}}_t \\ &= A(\hat{q}_t)(\vec{y}'_{\mathrm{A},t} + \vec{w}_{\mathrm{A},t}) - A(\hat{q}_t)A(\delta q_t)(\vec{y}'_{\mathrm{A},t} - \vec{w}_{\mathrm{A},t}) \\ &\approx A(\hat{q}_t)\left[\mathbf{I_3} - A(\delta q_t)\right]\vec{y}'_{\mathrm{A},t} + A(\hat{q}_t)\vec{w}_{\mathrm{A},t}.\end{aligned} \tag{20}$$

The direction cosine matrix for a small error quaternion δq_t can be approximated by

$$A(\delta q_t) \approx \begin{bmatrix} 1 & -2\delta q_{t,3} & 2\delta q_{t,2} \\ 2\delta q_{t,3} & 1 & -2\delta q_{t,1} \\ -2\delta q_{t,2} & 2\delta q_{t,1} & 1 \end{bmatrix}, \tag{21}$$

thus we can get

$$\begin{aligned}\dot{\delta\vec{v}}_t &= -2A(\hat{q}_t)\delta\vec{q}_t \times \vec{y}'_{\mathrm{A},t} + A(\hat{q}_t)\vec{w}_{\mathrm{A},t} \\ &= 2A(\hat{q}_t)\left[\vec{y}'_{\mathrm{A},t}\times\right]\delta\vec{q}_t + A(\hat{q}_t)\vec{w}_{\mathrm{A},t}.\end{aligned} \tag{22}$$

For relatively short time intervals, the dynamics of the error velocity can be written as

$$\delta\vec{v}_t = \delta\vec{v}_{t-1} + 2\Delta t A(\hat{q}_t)\left[\vec{y}'_{\mathrm{A},t}\times\right]\delta\vec{q}_{t-1} + \vec{u}_{\mathrm{A},t} \tag{23}$$

where $\vec{u}_{\mathrm{A},t} = A(\hat{q}_t)\vec{w}_{\mathrm{A},t}$ is a zero mean Gaussian noise, with covariance matrix Q_{v}.

3) Position error model: The dynamics of the error position is straightforward:

$$\delta\vec{p}_t = \delta\vec{p}_{t-1} + \Delta t\delta\vec{v}_t + \vec{u}_{\mathrm{p},t} \tag{24}$$

where $\vec{u}_{\mathrm{p},t}$ is a zero mean Gaussian noise, with covariance matrix Q_{p}. From (7), (17), (9), (23) and (24), we can get $\mathbf{F}_t$ as

$$\mathbf{F}_t = \begin{bmatrix} \mathbf{I_3} + \Delta t\,[\vec{y}_{\mathrm{G},t}\times] & -\frac{1}{2}\Delta t\mathbf{I_3} & \mathbf{0} & \mathbf{0} & \mathbf{0} \\ \mathbf{0} & \mathbf{I_3} & \mathbf{0} & \mathbf{0} & \mathbf{0} \\ \mathbf{0} & \mathbf{0} & \mathbf{I_3} & \Delta t\mathbf{I_3} & \mathbf{0} \\ 2\Delta t A(\hat{q}_t)\left[\vec{y}'_{\mathrm{A},t}\times\right] & \mathbf{0} & \mathbf{0} & \mathbf{I_3} & \mathbf{0} \\ \mathbf{0} & \mathbf{0} & \mathbf{0} & \mathbf{0} & \mathbf{I_3} \end{bmatrix} \tag{25}$$

where $\mathbf{0}$ is a 3×3 matrix of zeros. It is assumed that the noise for each state variable is uncorrelated with the noise for each other state. Hence, all non-diagonal terms of the noise matrix Q are zero and $Q = diag\left(Q_{\mathrm{q}}, Q_{\mathrm{bG}}, Q_{\mathrm{p}}, Q_{\mathrm{v}}, Q_{\mathrm{bA}}\right)$ for the big CKF and $Q = diag\left(Q_{\mathrm{q}}, Q_{\mathrm{bG}}\right)$ for the small CKF.

The measurement model of the proposed method is governed by

$$\delta\vec{z}_t = \mathbf{O_t}\delta x_t + \vec{n}_t \tag{26}$$

where $\delta\vec{z}_t$ is the error measurement, $\vec{n}_t$ is the measurement Gaussian noise with covariance matrix $R = E\left(\vec{n}_t\vec{n}_t^{\mathrm{T}}\right)$, which

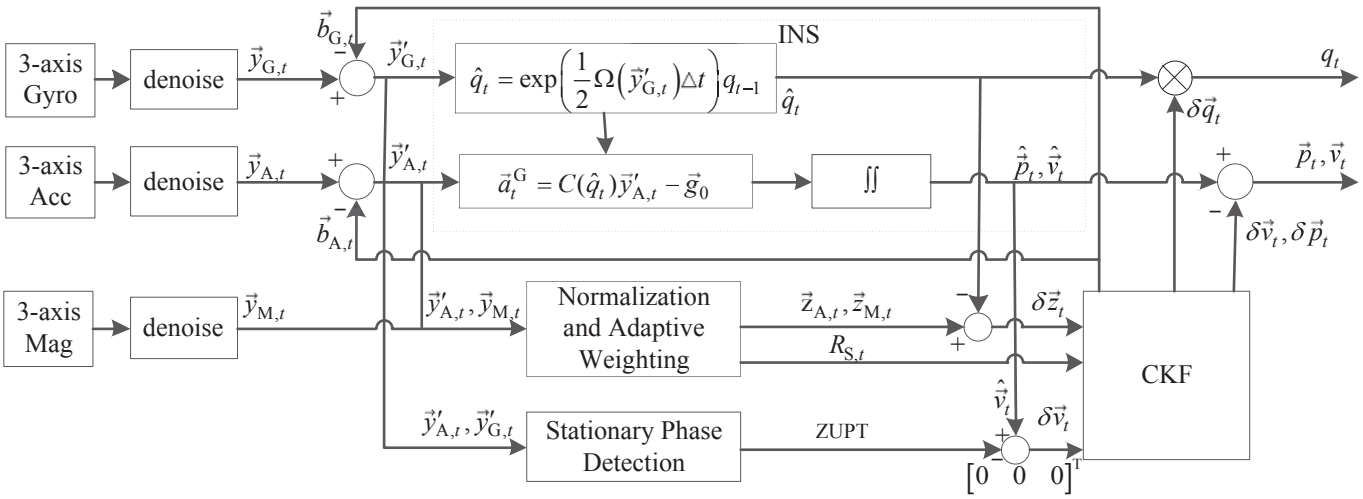

Fig. 2. The flowchart of the CKF for orientation and displacement estimation. 3-axis acc, gyro and mag represent the 3-axis signals from the three types of sensors. Orientation $\hat{q}_t$ and position $\hat{\vec{p}}_t$ are estimated based on INS. The difference between the accelerometer and magnetometer measurements and the gyroscope-based accelerometer and magnetometer measurements are used by CKF which estimates the errors of state. When foot is stationary on the ground, the error between the estimated velocity and zero velocity is also used as the input of CKF. The error state of the CKF are used to compensate acceleration, angular rate, orientation velocity and position estimates resulting in $\vec{y}'_{\mathrm{A},t}$, $\vec{y}'_{\mathrm{G},t}$, q_t, $\vec{v}_t$, and $\vec{p}_t$. The measurement noise covariance matrix $R_{\mathrm{S,t}}$ is adaptively adjusted to compensate for magnetic and body acceleration disturbances.

is assumed to be uncorrelated with the process noise, and $\mathbf{O_t}$ is the measurement matrix, which needs to be determined. The error input to the CKF is the difference between the true and estimated data provided by accelerometer and magnetometer in the sensor frame. Given the last estimate of the quaternion q_{t-1}, by applying (1), the current predicted quaternion $\hat{q}_t$ can be obtained. Given the normalized gravity vector $\vec{r}_{\mathrm{A}}$ and the earth magnetic vector $\vec{r}_{\mathrm{M}}$ in the global frame, the relation between the true and estimated gravity vector and the earth magnetic vector in the sensor frame can be expressed as

$$\begin{aligned}\vec{r}'_{\mathrm{A},t} &= A^{\mathrm{T}}(q_t)\vec{r}_{\mathrm{A}} = A^{\mathrm{T}}(\delta q_t)A^{\mathrm{T}}(\hat{q}_t)\vec{r}_{\mathrm{A}} = A^{\mathrm{T}}(\delta q_t)\hat{\vec{z}}_{\mathrm{A},t}\\ \vec{r}'_{\mathrm{M},t} &= A^{\mathrm{T}}(q_t)\vec{r}_{\mathrm{M}} = A^{\mathrm{T}}(\delta q_t)A^{\mathrm{T}}(\hat{q}_t)\vec{r}_{\mathrm{M}} = A^{\mathrm{T}}(\delta q_t)\hat{\vec{z}}_{\mathrm{M},t}\end{aligned} \tag{27}$$

where $\vec{r}'_{\mathrm{A},t}$ and $\vec{r}'_{\mathrm{M},t}$ are the normalized gravity and earth magnetic vector in the BCS, $\hat{\vec{z}}_{\mathrm{A},t}$ and $\hat{\vec{z}}_{\mathrm{M},t}$ are the gyroscope-based estimated normalized gravity and earth magnetic vector in the BCS. The error measurement input to the CKF is got from

$$\begin{aligned}\begin{bmatrix}\delta\vec{z}_{\mathrm{A},t}\\ \delta\vec{z}_{\mathrm{M},t}\end{bmatrix} &= \begin{bmatrix}\vec{z}_{\mathrm{A},t} - \hat{\vec{z}}_{\mathrm{A},t}\\ \vec{z}_{\mathrm{M},t} - \hat{\vec{z}}_{\mathrm{M},t}\end{bmatrix}\\ &= \begin{bmatrix}\vec{r}'_{\mathrm{A},t} + \frac{\vec{a}_t + \vec{b}_{\mathrm{A},t} + \vec{w}_{\mathrm{A},t}}{g_0} - \hat{\vec{z}}_{\mathrm{A},t}\\ \vec{r}'_{\mathrm{M},t} + \frac{\vec{d}_{\mathrm{M},t} + \vec{w}_{\mathrm{M},t}}{m_0} - \hat{\vec{z}}_{\mathrm{M},t}\end{bmatrix}\\ &\approx \begin{bmatrix}\vec{r}'_{\mathrm{A},t} - \hat{\vec{z}}_{\mathrm{A},t}\\ \vec{r}'_{\mathrm{M},t} - \hat{\vec{z}}_{\mathrm{M},t}\end{bmatrix} + \begin{bmatrix}\frac{\vec{w}_{\mathrm{A},t}}{g_0}\\ \frac{\vec{w}_{\mathrm{M},t}}{m_0}\end{bmatrix}\\ &= \begin{bmatrix}A^{\mathrm{T}}(\delta q_t) - \mathbf{I_3}\\ A^{\mathrm{T}}(\delta q_t) - \mathbf{I_3}\end{bmatrix}\begin{bmatrix}\hat{\vec{z}}_{\mathrm{A},t}\\ \hat{\vec{z}}_{\mathrm{M},t}\end{bmatrix} + \begin{bmatrix}\frac{\vec{w}_{\mathrm{A},t}}{g_0}\\ \frac{\vec{w}_{\mathrm{M},t}}{m_0}\end{bmatrix}\\ &= 2\begin{bmatrix}[\hat{\vec{z}}_{\mathrm{A},t}\times]\\ [\hat{\vec{z}}_{\mathrm{M},t}\times]\end{bmatrix}\delta\vec{q}_t + \begin{bmatrix}\frac{\vec{w}_{\mathrm{A},t}}{g_0}\\ \frac{\vec{w}_{\mathrm{M},t}}{m_0}\end{bmatrix}\end{aligned} \tag{28}$$

where g_0 and m_0 are magnitude of the gravity and earth magnetic vector respectively. (28) only holds when $\vec{a}_t$ and $\vec{d}_{\mathrm{M},t}$ can be ignored compared to g_0 and m_0, respectively. When the sensor node is stationary, the error velocity vector $\delta\vec{v}_t$ can be taken as the third error measurement, which can be calculated for ZUPT as $\delta\vec{v}_t = \hat{\vec{v}}_t - \begin{bmatrix}0 & 0 & 0\end{bmatrix}^{\mathrm{T}}$. To sum up, if ZUPT condition satisfies, the measurement function of the CKF can be modeled as

$$\delta\vec{z}_t = \begin{bmatrix}2[\hat{\vec{z}}_{\mathrm{A},t}\times] & \mathbf{0} & \mathbf{0} & \mathbf{0} & \mathbf{0}\\ 2[\hat{\vec{z}}_{\mathrm{M},t}\times] & \mathbf{0} & \mathbf{0} & \mathbf{0} & \mathbf{0}\\ \mathbf{0} & \mathbf{0} & \mathbf{0} & \mathbf{I_3} & \mathbf{0}\end{bmatrix}\delta x_t + \vec{n}_t, \tag{29a}$$

or else

$$\delta\vec{z}_t = \begin{bmatrix}2[\hat{\vec{z}}_{\mathrm{A},t}\times] & \mathbf{0} & \mathbf{0} & \mathbf{0} & \mathbf{0}\\ 2[\hat{\vec{z}}_{\mathrm{M},t}\times] & \mathbf{0} & \mathbf{0} & \mathbf{0} & \mathbf{0}\end{bmatrix}\delta x_t + \vec{n}_t. \tag{29a}$$

Gravity and earth magnetic direction are used to correct the estimated quaternion. However, body acceleration interferences and magnetic disturbances will decrease the accuracy of the estimated orientations. Thus, the confidence of these two types of data source needs to be determined before used for correction. An adaptive weighting mechanism is proposed by adjusting measurement noise covariance matrix $R_{\mathrm{S,t}}$ to preclude the body acceleration and magnetic disturbances from influencing the filter behavior. The implementation details of adaptive weighting can be found in [11].

During the movement of walking, running and hopping, there is a phase in which the foot stays still on the ground. For walking, the foot flat phase during the stance is detected to apply ZUPT. This phase is ensured to last for about 0.3 seconds. For running, the still time is much shorter than walking, and there is a phase in which both feet leave ground.

The still time of running is detected by the sharp spikes on heel strike. Actually it is challenging to detect the stationary phase of running. The foot stays stationary for a much shorter time during running than walking, and for fast speed running, there is no such stationary phase at all. The foot stationary detection relies on basic signal processing techniques with accelerometers or gyroscopes. For different gait patterns, the detection of foot stationary is obtained by tuning the threshold of the sensor signals.

A standard Kalman filter is employed to deal with the filtering [12]. After CKF measurement update, we will correct the previously predicted orientation, velocity and position at time step t using the updated CKF error state through the following equations:

$$\begin{aligned} q_t &= \hat{q}_t \otimes \delta q_t = \begin{bmatrix} \Xi(\hat{q}_t) & \hat{q}_t \end{bmatrix} \begin{bmatrix} \delta\vec{q}_t \\ 1 \end{bmatrix} = \Xi(\hat{q}_t)\delta\vec{q}_t + \hat{q}_t \\ \vec{v}_t &= \hat{\vec{v}}_t - \delta\vec{v}_t \\ \vec{p}_t &= \hat{\vec{p}}_t - \delta\vec{p}_t, \end{aligned} \tag{30}$$

where $\Xi(\hat{q}_t) = \begin{bmatrix} [\vec{e}\times] + q_{t,4}\mathbf{I_3} \\ -\vec{e}_t^{\mathrm{T}} \end{bmatrix}$. The error state is reset to zero after being used in INS to refine the current orientation, velocity and position. The bias terms i.e. gyroscope and accelerometer biases are maintained over time in the CKF.

C. Biomechanical fusion

When we get the orientations of the SMUs relative to the global frame, denoted as q^{GS}, sensor to body calibration needs to be performed to get the orientations of the body segments in the global frame, denoted as q^{GB}. The details of sensor to segment calibration can be seen in [10]. A fusion method is proposed to get the CoM displacement based on the linked biomechanical model as shown in Fig. 3. The right CoM positions will be taken for example to show the calculation process. Constitute two sets of the right lower limb segments and the right lower limb joints, $\mathrm{S}=\{\mathrm{Rpelvis}, \mathrm{Rfemur}, \mathrm{Rtibia}, \mathrm{Rfoot}\}$, and $\mathrm{J}=\{\mathrm{RCoM}, \mathrm{Rhip}, \mathrm{Rknee}, \mathrm{Rankle}, \mathrm{Rtoe}\}$. The right CoM positions can be obtained according to the following equations:

$$\vec{p}_{\mathrm{J}_{i-1},t} = \vec{p}_{\mathrm{J}_i,t} - q^{\mathrm{GB}}_{\mathrm{S}_{i-1},t} \otimes \vec{l}_{\mathrm{S}_{i-1},0} \otimes \left(q^{\mathrm{GB}}_{\mathrm{S}_{i-1},t}\right)^{-1} \tag{31}$$

where $i = 5, 4, 3, 2$, respectively, are the elements indexes of the two sets. $\vec{l}_{\mathrm{S}_{i-1},0}$ is the initial vector representing the lower body segments, which should be measured before calculation. $q^{\mathrm{GB}}_{\mathrm{S}_{i-1},t}$ are the orientations of the lower body segments at time step t during the movements, which rotate the initial vectors of the body segments in the GCS. $\vec{p}_{\mathrm{J}_i,t}$ represents the positions of the lower body joints in the GCS.

From biomechanical fusion, we can obtain two positions of the CoM from each lower limb at time step t, denoted by $\vec{p}^{\,\mathrm{L}}_{\mathrm{CoM}}$ and $\vec{p}^{\,\mathrm{R}}_{\mathrm{CoM}}$, respectively. Constituting a new state vector $\vec{s}_t$ of $\vec{p}^{\,\mathrm{L}}_{\mathrm{CoM}}$ and $\vec{p}^{\,\mathrm{R}}_{\mathrm{CoM}}$, i.e. $\vec{s}_t = \begin{bmatrix} \vec{p}^{\,\mathrm{L}}_{\mathrm{CoM},t}, \vec{p}^{\,\mathrm{R}}_{\mathrm{CoM},t} \end{bmatrix}^{\mathrm{T}}$. Statistically, the two left/right CoM positions got from each lower limb are supposed to be the same. The relation of the two left/right CoM positions can be expressed as in a linearized function:

$$\vec{\varepsilon}_{\mathrm{p},t} = \mathbf{U}\vec{s}_t + \vec{\mu}_{\mathrm{p},t} \tag{32}$$

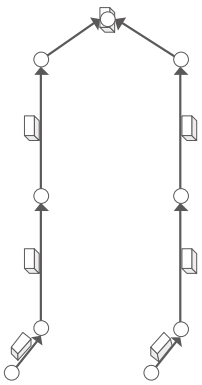

Fig. 3. The biomechanical model of the human lower body. The circles are the joints; the lines with arrow indicate the body segments, and the arrow shows the kinematic propagation direction in the lower body model; and the cubes represent the SMUs placed on the segments.

where $\vec{\mu}_{\mathrm{p},t}$ is the measurement noise, which is supposed to be Gaussian noise. The measurement $\vec{\varepsilon}_{\mathrm{p},t}$ is supposed to be zero and the measurement matrix $\mathbf{U}$ is given by

$$\mathbf{U} = \begin{bmatrix} \mathbf{I_3} & -\mathbf{I_3} \end{bmatrix} \tag{33}$$

Another Kalman filter is adopted to reduce the CoM position error. Because Kalman filter implements in a prediction-update way at each time step, the dynamical model is given by a random walk model of the state variable which is represented as

$$\vec{s}_t^{\,*} = \vec{s}_t^{\,-} + \vec{\eta}_t \tag{34}$$

where $\vec{s}_t^{\,-}$ contains the two estimated CoM positions got from biomechanical fusion, $\vec{s}_t^{\,*}$ is the predicted position vector, and $\vec{\eta}_t$ is the process noise and is also assumed to be a Gaussian vector. Then the CoM position is updated by

$$\vec{s}_t^{\,+} = \vec{s}_t^{\,*} + K_t(\vec{\varepsilon}_{\mathrm{p},t} - \mathbf{U}\vec{s}_t^{\,-}) \tag{35}$$

where $\vec{s}_t^{\,+}$ is the CoM positions after the Kalman update and K_t is the Kalman gain.

D. Ground contact update

During biomechanical fusion, ground contact update is introduced. The external contact is used to further limit the boundless integration error of the foot position. It makes use of the fact that under most circumstances, it can be assumed that human body must be in contact with a flat ground, and thus the vertical position of the joint in contact with the ground is supposed to be zero. Fig. 4 shows the ground contact information of walking, running and hopping. When the signal, which can be the accelerometer or gyroscope measurements, is high, the foot leaves the ground, and when the signal is low, the foot is in contact with the ground. The solid line stands for right foot, and dashed line is for left foot. During the walking gait cycle, there is always at least one foot in contact with the ground. During the double support phase, both feet are in contact with the ground. For running, there is a phase in which both feet leave the ground. For hopping, both feet leave

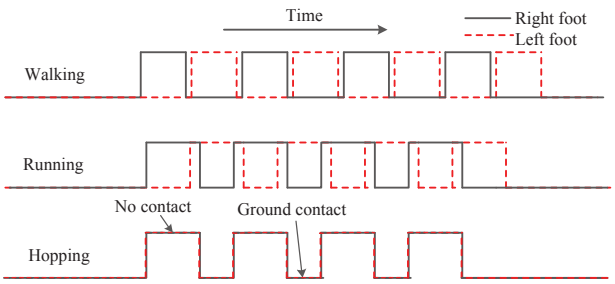

Fig. 4. The ground contact information of walking, running and hopping. When the signal is high, it means that foot leaves the ground; when low, the foot is in contact with the ground. The solid line shows the contact info. of the right foot, and the dashed line gives the contact info. of the left foot during walking, running and hopping, respectively.

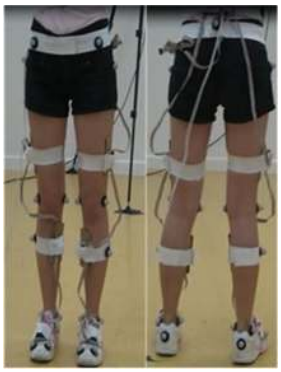

Fig. 5. The attachment of the optical markers and 7 SMUs to the human lower body. The optical markers are placed on the joints to get the position and orientation of each segment to provide ground truth of the fusion results from the measurement of the SMUs.

ground or fall to the ground at the same time. It is much easier to detect the ground contact phase for hopping.

Ground contact information is detected using the hypothesis testing. It is supposed that when the foot is stationary on the ground, the accelerometer only measures the gravitational acceleration, so the norm of the accelerometer measurements should be equal to g_0. The null hypothesis is defined as joint $j \in \mathrm{J_{ref}}$ is stationary at time step t, which can be described as

$$H_{0_j,t}: \ \varphi_{\mathrm{A},t} = g_0, \ j \in \mathrm{J_{ref}} \tag{36}$$

where $\mathrm{J_{ref}}$ is defined as the set of the entire potential reference joints which are in contact with the ground, and in this paper, this set includes left toe and right toe. $\varphi_{\mathrm{A},t}$ is the l^2-norm of the accelerometer signals $\vec{y}_{\mathrm{A},t}$.

The statistic used for the test is the absolute value difference between the norm of the accelerometer signal and the norm of the gravitational acceleration, defined by

$$d_{j,t} = \left|\varphi_{\mathrm{A},t} - g_0\right|. \tag{37}$$

The probability of $H_{0_j,t}$, denoted by $P\left(H_{0_j,t}\right)$ is calculated with

$$P\left(H_{0_j,t}\right) = P\left(\varphi_{\mathrm{A},t}|g_0\right) = 2\Phi\left(-d_{j,t}\right) \tag{38}$$

where Φ is the cumulative distribution function of the standard normal distribution. When the foot stays stationary on the ground, the probability is 1, and when the foot swings in the air, the probability is 0. The threshold should be defined to determine if the foot is in contact with the ground.

III. Experimental Results and Performance Evaluation

The MMocap system for the lower body consists of 7 SMUs. Each SMU contains a tri-axis accelerometer, a tri-axis gyroscope and a tri-axis magnetometer. These SMUs are connected to a base station by data buses. The base station sends data packets via a high-speed wireless module to PC for data processing. The sampling rate of the MMocap system is 100Hz. The SMUs are fixed on the human lower body segments tightly using elastic straps. Meanwhile, optical markers for the laboratory bound Osprey optical motion analysis system are placed on the joints of human lower body (pelvis, hips, knees, ankles and toes). The Osprey system consists of 6 video cameras operating at 100Hz. The position of the markers and SMUs attached to the human lower body are shown in Fig. 5. To validate the performance of the proposed algorithm, experiments including walking, running and hopping are carried out in the capture volume of the reference optical system. The subject conducts each experiment for 5 times at a comfortable speed. There is no defined path for each experiment. The subject can walk/run forwards, backwards and sideways at will and make turns freely. The accuracy of the displacement of the root joint is quantified by calculating the Root Mean Square Error (RMSE) with respect to the ground truth provided by the optical system. From each sensor readings, we can get an orientation represented by a quaternion at each time step. After sensor to segment calibration, the orientations for each segment can be obtained. Taking the root joint for example, the estimated orientations for running gait are shown in Fig. 6. The dashed line is the ground truth provided by optical system. The dot-dashed line is the orientation obtained by integrating the angular rate signal from the pelvis. The solid line is the estimation results using our proposed method. From Fig. 6, our method achieves good accuracy in orientation estimation compared to the ground truth provided by the optical system. The estimated displacements for walking, running and hopping are shown in Fig. 7, 8 and 9, respectively. In each figure, the dashed line is the reference displacement provided by the optical system. The solid line shows the displacement estimated by our proposed method. The the dotted-dashed line is the CoM displacements obtained by double integration of the accelerometer measurements placed on the pelvis after removing gravity components. It should be noted that the initial position is subtracted from the reference position to compare with the estimated displacements. From Fig. 7, 8 and 9, the integration method can only get accurate CoM displacement for a very short time period, and the drifts in the displacement increase over time. In general, the estimated CoM displacement by our proposed method is quite similar to the results of the optical Osprey system, which means that our proposed method can estimate the CoM displace-

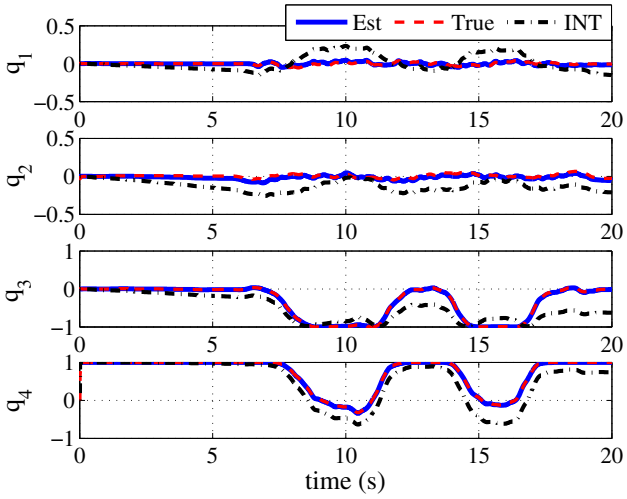

Fig. 6. The orientations of the root joint represented by quaternion in the global coordinate system for running. Solid line: our method; dashed line: the ground truth; dot-dashed line: integration method.

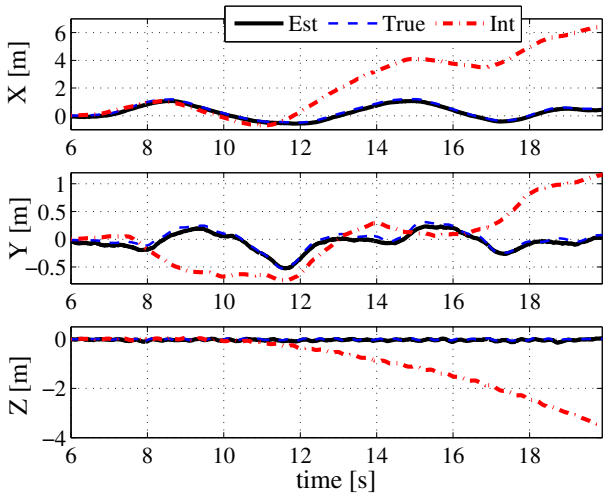

Fig. 8. The CoM displacement of running (upper: X, middle: Y, lower: Z). Solid line: The CoM displacement after geometric fusion; dashed line: the ground truth; dot-dashed line: integration method.

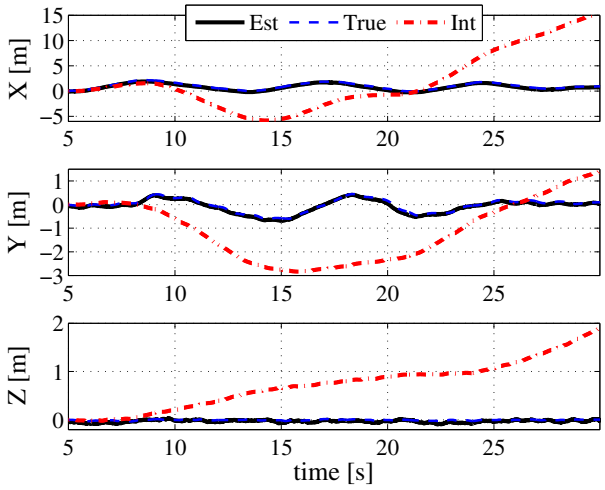

Fig. 7. The CoM displacement of walking (upper: X, middle: Y, lower: Z). Solid line: The estimated CoM displacement; dashed line: the ground truth; dot-dashed line: integration method.

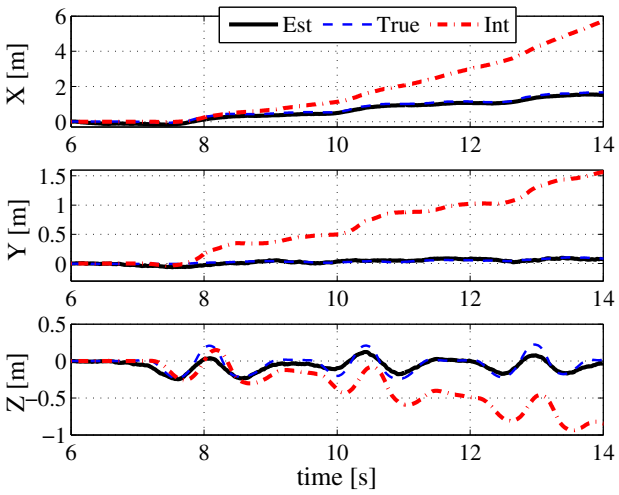

Fig. 9. The CoM displacement of hopping (upper: X, middle: Y, lower: Z). Solid line: The CoM displacement after geometric fusion; dashed line: the ground truth; dot-dashed line: integration method.

ment accurately for different gait patterns of walking with high accuracy. The average RMS errors and their standard deviations (RMSE±SD) of the displacement for each gait calculated over 5 trials are given in Table I. From Table I, the RMSE values of our method are much smaller compared to the RMS errors of the displacement got from the double integration of the acceleration of the pelvis. It means that the accuracy of our method to estimate the displacement is improved a lot. However, for running, the RMS error is still higher than walking which is because during running, the stationary phase is quite short, so it is more difficult to detect this phase correctly compared to walking and hopping.

Based on our proposed algorithm, the foot displacement should be obtained first. To get the foot displacement, the acceleration in the global coordinate system should be calculated using the orientations of the sensor placed on the feet. To get the CoM displacement using the biomechanical model, the orientations of the lower body segments are needed. Thus, the major cause of the displacement error comes from the orientation estimates. Two possible explanations for the orientation errors are described. Firstly, the earth magnetic field is used for the drift correction around the vertical axis of the orientation. Due to the experiments are conducted in the indoor environment, the structural beam in the building and electronic devices around may distort the magnetic field strongly. The high level magnetic disturbances would cause orientations error. Compensation of magnetic disturbances should be done to improve the orientations of the human

TABLE I

THE COM DISPLACEMENT RMS ERRORS AND THEIR STANDARD DEVIATIONS ON EACH AXIS BETWEEN THE GROUND TRUTH AND ESTIMATED DISPLACEMENT OF WALKING, RUNNING AND HOPPING. EACH EXPERIMENT ARE PERFORMED 5 TIMES. PROVIDED BY OUR PROPOSED METHOD (EST) AND INTEGRATION METHOD (INT)

RMSE±SD(m)	walking		running		hopping	
	Est	Int	Est	Int	Est	Int
X	0.08±0.02	3.56±0.89	0.12±0.05	5.73±1.39	0.09±0.03	1.56±0.75
Y	0.05±0.03	4.01±0.76	0.10±0.02	6.05±1.76	0.04±0.03	1.98±0.73
Z	0.04±0.01	2.29±0.58	0.06±0.03	3.11±0.74	0.08±0.02	2.31±0.95

body segments. Secondly, the gravitational acceleration is used to provide inclination stability of the orientation estimations. However, accelerometer measures the vector sum of the body acceleration and gravitational acceleration. When gravitational vector is used for inclination correction, the body accelerations are the disturbances to the gravitational vector. To improve the accuracy of the orientations, efforts should be taken to eliminate the deleterious effects caused by the disturbances of the body acceleration. Sun *et al.* [13] proposed a method to estimate the acceleration caused by human movements by modeling the human acceleration as a first-order Markov process, and subtracted it from the accelerometer signals before it is used for correction. The accuracy of the orientation was improved after removing motion acceleration from the accelerometer measurements. To further improve the accuracy of the system, removing the acceleration caused by human motions from the gravitational acceleration is considered as our future work.

IV. CONCLUSION

This paper proposes a self-contained displacement estimation method to estimate the CoM displacement for MMocap system. The method works without any additional external supporting infrastructures, such as magnetic, UWB or GPS. A CKF which operates on the errors of the state variables using a feedback structure is designed to estimate the orientations of the lower body segments as well as the displacements of both feet. The CoM displacement can then be acquired by further fusion of the lower body orientations and feet locations based on the linked biomechanical model. From the experimental results, our method can accurately capture human motion including orientation and locomotion for these three different gait patterns, e.g. walking, running, and hopping with regard to the optical motion tracker. Further improvements are expected in our work. The threshold used to detect the foot stationary phase for ZUPT has to be manually tuned to get the right information for different gaits. For real-time system, we have to detect this phase adaptively.

ACKNOWLEDGMENT

This research is part of CSIDM Project No.CSIDM-200802, partially supported by project grant reference number MDA(R)2/4-1(C) from the Interactive and Digital Media Project Office (IDMPO) administered by the Media Development Authority (MDA) of Singapore and partially funded by National Natural Science Foundation of China (Grant No. 60932001).

REFERENCES

[1] R. Zhu and Z. Zhou, "A real-time articulated human motion tracking using tri-axis inertial/magnetic sensors package," *IEEE Trans. Neural Syst. Rehabil. Eng.*, vol. 12, no. 2, pp. 295–302, 2004.

[2] D. Vlasic, R. Adelsberger, G. Vannucci, J. Barnwell, M. Gross, W. Matusik, and J. Popović, "Practical motion capture in everyday surroundings," *ACM Trans. Graph.*, vol. 26, no. 3, pp. 35:1–35:9, 2007.

[3] H. Schepers and P. Veltink, "Stochastic magnetic measurement model for relative position and orientation estimation," *Meas. Sci. Technol.*, vol. 21, no. 6, p. 065801, 2010.

[4] Z. Zhang, W. Wong, and J. Wu, "Ubiquitous human upper-limb motion estimation using wearable sensors," *IEEE Trans. Inf. Technol. Biomed.*, vol. 15, no. 4, pp. 513–521, 2011.

[5] X. Meng, S. Sun, L. Ji, J. Wu, and W. Wong, "Estimation of center of mass displacement based on gait analysis," in *Proc. 8th Int. Conf. Body Sensor Networks (BSN'11)*, Dallas, Texas, May 2011, pp. 150–155.

[6] K. Yamanaka, M. Kanbara, and N. Yokoy, "Localization of walking or running user with wearable 3d position sensor," in *Proc. 17th Int. Conf. Artificial Reality and Telexistence (ICAT'07)*, Esbjerg, Denmark, 2007, pp. 39–45.

[7] A. Young, "From posture to motion: the challenge for real time wireless inertial motion capture," in *Proc. 5th Int. Conf. Body Area Networks (BodyNets'10)*, Corfu, Greece, 2010, pp. 1–7.

[8] X. Yun, E. Bachmann, H. Moore, and J. Calusdian, "Self-contained position tracking of human movement using small inertial/magnetic sensor modules," in *Proc. 2007 IEEE Int. Conf. Robot. Autom. (ICRA'07)*, Roma, Italy, 2007, pp. 2526–2533.

[9] D. Choukroun, I. Bar-Itzhack, and Y. Oshman, "Novel quaternion kalman filter," *IEEE Trans. Aero. Elec. Sys.*, vol. 42, no. 1, pp. 174–190, 2006.

[10] X. Meng, Z. Zhang, S. Sun, J. Wu, and W.Wong, "Biomechanical model-based displacement estimation in micro-sensor motion capture," *Meas. Sci. Technol.*, vol. 23, no. 5, p. 055101, 2012.

[11] S. Sun, X. Meng, L. Ji, J. Wu, and W. Wong, "Adaptive sensor data fusion in motion capture," in *Proc. 13th Int. Conf. Inf. Fusion (FUSION'10)*, Edinburgh, U.K., 2010, pp. 1–8.

[12] G. Welch and G. Bishop, "An introduction to the kalman filter," Univ. North Carolina, Chapel Hill, CMPSCI Tech. Rep., 2002.

[13] S. Sun, X. Meng, L. Ji, Z. Huang, and J. Wu, "Adaptive kalman filter for orientation estimation in micro-sensor motion capture," in *Proc. 14th Int. Conf. Inf. Fusion (FUSION'11)*, Chicago, Illinois, USA., 2011, pp. 1–8.